7604 *Macromolecules* **2010**, *43*, 7604–7610
DOI: 10.1021/ma101313m

Macromolecules
ARTICLE

Highly Oriented and Nanotextured Films of Regioregular Poly(3-hexylthiophene) Grown by Epitaxy on the Nanostructured Surface of an Aromatic Substrate

Martin Brinkmann,*,† Christophe Contal,† Navaphun Kayunkid,† Tatjana Djuric,‡ and Roland Resel‡

†*Institut Charles Sadron, CNRS- University of Strasbourg, 23 rue du loess, 67034 Strasbourg, France, and* ‡*Institute of Solid State Physics, Petersgasse 16, 8010 Graz, Austria*

Received June 14, 2010; Revised Manuscript Received August 9, 2010

ABSTRACT: A simple method for the nanotexturing and orientation of regioregular poly(3-hexylthiophene) (P3HT) thin films has been developed. Epitaxial growth of P3HT on the surface of an aromatic salt (potassium 4-bromobenzoate) (K−BrBz) leads to highly oriented and nanotextured P3HT films which consist of a regular network of interconnected semicrystalline domains oriented along two preferential in-plane directions. The overall crystallinity and the level of in-plane orientation of the P3HT films are controlled by the temperature of isothermal crystallization (T_{iso}). Well-defined electron diffraction patterns with sharp reflections obtained for $T_{iso} = 180$ °C indicate that the crystalline domains grow with a unique (1 0 0) P3HT contact plane on the K−BrBz substrate with the P3HT chains oriented along the [0 ±2 1] K−BrBz directions of the substrate. During the annealing of the polymer film, the surface of the aromatic salt undergoes a topographic reconstruction resulting in a regular nanostructured "hill and valley" topography that templates and orients the growth of P3HT. Preferred orientation of P3HT crystalline domains occurs at step edges of the substrate and is favored by the matching between the layer period of P3HT and the terrace height of the K−BrBz substrate.

I. Introduction

Semiconducting polymers belong to one of the most interesting class of functional materials and are now widely used in plastic electronics for the fabrication of electronic devices.[1] Among the numerous semiconducting conjugated polymers, regioregular poly(3-alkylthiophene)s (P3ATs) have attracted much interest as they combine facile processability and high charge carrier mobilities useful in the elaboration of Organic Field Effect Transistors (OFETs) and polymer solar cells (PSCs).[2] Nanostructuring of conjugated polymers is relevant for a number of emerging applications in the field of plastic electronics e.g. photovoltaics and ambipolar charge transport.[3,4] For instance, in the case of photovoltaics, nanostructuring of a donor−acceptor system results in a large interfacial area between electron-donnor and electron-accepting components, which is necessary to optimize the charge separation of the photogenerated excitons. Various approaches have been developed to achieve controlled nanostructuring on the 10 nm-100 nm length scale in conjugated polymers and molecular materials. An elegant approach is based on the synthesis of self-assembling block copolymers bearing electron-accepting and electron-donating groups that undergo phase separation.[5] Nanostructuring may also be obtained by controlling the length-scale of macrophase separation via surface-directed demixing of a donor conjugated/guest polymer blend during spin coating.[6] Alternatively, "nanoimprint lithography" (also termed embossing) or "wet lithography" methods can also provide large areas of nanopatterned films.[7,8] Whereas regular nanostructured films are obtained by these methods, preferential in-plane orientation of highly crystalline features is more difficult to reach although some orientation of crystalline polyfluorene has been reported by Jonas and co-workers.[9] Nevertheless, such a preferential orientation of the P3HT crystallites is highly desirable in thin films as charge transport is particularly anisotropic in π-conjugated semi-conductors like P3HT. In the case of P3HT for instance, the charge mobility along the polymer chain direction is one order of magnitude larger than perpendicular to it.[10] In this context, epitaxy of semi-crystalline polymers on aromatic organic crystals is an original and elegant method to grow highly crystalline and oriented polymer thin films with a controlled and regular nanostructured morphology.[11−16] Brinkmann and coworkers have demonstrated the high potential of epitaxial crystallization in terms of morphology control, nanostructuring and structure determination for poly(3-alkylthiophene)s and poly(dialkylfluorene)s. More generally, epitaxy of semi-crystalline polymers can be realized on a large variety of aromatic molecular crystals.[17−20] For instance, *p*-terphenyl and anthracene lead to highly oriented polymer films of polyethylene (PE) when the growth is performed on the surface of uniform single crystals of these aromatic molecules. The epitaxial conditions often impose the lamellae to grow in such a way that the polymer chains are oriented along given crystallographic directions in the plane of the substrate. For instance, the chains of P3HT are aligned along the stacking direction of 1,3,5-trichlorobenzene molecules during the process of directional epitaxial crystallization.[11] Frequently, crystalline lamellae of the polymer grow along two or more equivalent crystallographic orientations generating nanotextured patterns of highly interconnected chain-folded lamellae.[20]

In the present communication, we focus on the epitaxial growth of a key conjugated polymer, namely regioregular poly(3-hexylthiophene), on substrates of potassium 4-bromobenzoate (K−BrBz).

*Corresponding author. E-mail: martin.brinkmann@ics-cnrs.unistra.fr.

 Published on Web 08/25/2010

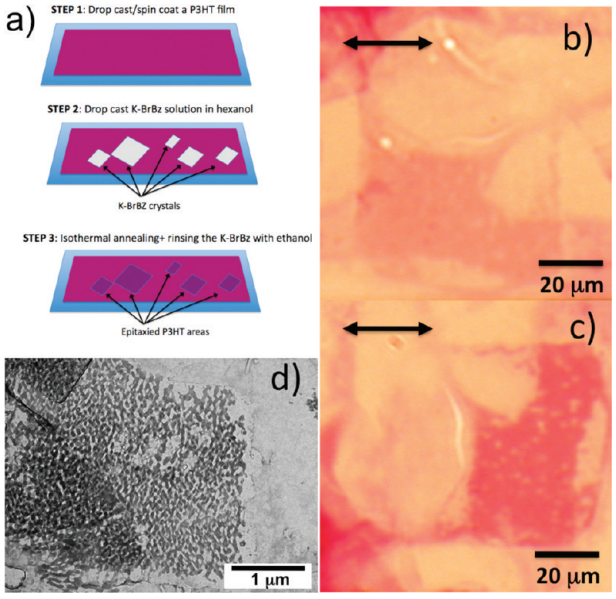

Figure 1. (a) Scheme illustrating the three main steps of the oriented P3HT thin film preparation method as described in the text (see Experimental Section). (b and c) POM images of an oriented area of P3HT grown epitaxially on K−BrBz at T = 180 °C. The K−BrBz crystals has been removed by rinsing with ethanol. The remaining epitaxied P3HT area has the initial lozenge shape of the K−BrBz crystal. The epitaxied P3HT area shows a variation of the absorbance vs orientation of the incident light polarization. (d) TEM bright field image showing an oriented and nanostructured P3HT film after removal of the K−BrBz substrate. Noteworthy, the shape of the oriented P3HT film matches the initial rhombic-shaped K−BrBz crystal.

Under proper isothermal crystallization conditions, epitaxial growth of P3HT on K−BrBz leads to highly crystalline, oriented and nanotextured films. The nanostructured morphology involves an interconnected network of semicrystalline P3HT domains (showing the periodic alternation of crystalline lamellae and amorphous zones) with a $(1\,0\,0)_{P3HT}$ contact plane and two preferred in-plane orientations of the P3HT chain axis. During the annealing of the polymer film on the K−BrBz substrate, a topographic "reconstruction" of the aromatic salt surface results in a nanostructured "hill and valley" morphology that templates and orients the growth of highly crystalline domains of P3HT.

II. Experimental Section

Potassium 4-bromobenzoate (K−BrBz) was prepared by reacting in a 1:1 molar ratio, 4-bromobenzoic acid (Aldrich) with a diluted potassium hydroxide solution (Aldrich) in ethanol. The material was subsequently purified by recrystallization in ethanol. The white powder was recovered and analyzed by X-ray diffraction (see Figure S1, Supporting Information). The diffraction pattern of the K−BrBz powder was measured with a Siemens D501 diffractometer in the focusing Bragg−Brentano geometry using Cu Kα radiation with a secondary graphite monochromator. Whole powder pattern decomposition using the LeBail method and subsequent indexation was performed with the TOPAS software. Analysis of the preferred orientation of the K−BrBz crystals on the P3HT film was performed by a texture goniometer. A Philips X'Pert system equipped with an ATC3 cradle was used with Cr Kα radiation and a secondary side graphite monochromator.

The epitaxial orientation of P3HT was performed by following the method illustrated in part a of Figure 1. In the first step, a thin film of P3HT was deposited on a clean glass slide (the cleaning procedure for the glass slides is described in details in reference 16) by using either the doctor blade method or a simple drop-casting of a 2 wt % solution of P3HT in chloroform (M_n = 18.8 kg/mol, M_w/M_n = 1.7, 96% regioregularity, Merck). The P3HT film thickness was in the range 30−50 nm as measured by atomic force microscopy (AFM). Large crystalline domains of K−BrBz were grown on top of the P3HT film by drop casting a 5 wt % solution of K−BrBz in hexanol. Upon evaporation of the solvent, large lozenge-shaped K−BrBz crystals were formed on the P3HT film surface as observed by Polarized Optical Microscopy (POM). Alternatively, the process can be modified in that the P3HT film can be deposited on top of the K−BrBz crystals. The P3HT samples on the K−BrBz substrate were transferred in a THMS-600 hot stage (Linkam) kept under nitrogen atmosphere for isothermal crystallization. Typical annealing procedures were as follow: First the temperature was raised to 240 °C to melt the polymer (1 min). Then the temperature was decreased to the temperature of isothermal crystallization in the range 160−220 °C for 10 h. Finally, the sample was rapidly cooled to room temperature at 20 °C/min. The annealed samples were subsequently rinsed with ethanol to remove the K−BrBz crystals. For transmission electron microscopy (TEM) analysis, highly oriented areas of P3HT were first identified by optical microscopy (Leica DMR-X microscope) using slightly decrossed polarizers (see Figure 1b,c). The epitaxied films of P3HT were carbon coated. The P3HT/carbon film was floated onto a diluted aqueous solution of HF (5% in weight) and recovered onto TEM copper grids. TEM was performed in bright and dark field modes using a CM12 Philips microscope equipped with a MVIII (Soft Imaging System) CCD camera. P3HT thin films were investigated by atomic force microscopy with a Nanoscope III in tapping mode using Si tips (25−50 N/m and 280−365 kHz). Image treatments (FFT) were performed by using the AnalySIS (Soft Imaging System) software.

III. Results

a. Preparation Method. The nanotexturing process via epitaxial growth on K−BrBz is illustrated schematically in Figure 1a. It involves three main steps: (i) preparing a P3HT film on a given substrate, (ii) growing K−BrBz crystals from a hot solution in hexanol on top the P3HT film and (iii) melting and isothermal crystallization of P3HT. Finally the K−BrBz crystals are easily removed by a rinse with ethanol.

The epitaxial growth described herein bears some similarity with the method of directional epitaxial crystallization of P3HT in 1,3,5-trichlorobenzene (TCB) in that the substrate used for the epitaxial crystallization and nanostructuring of P3HT is sacrificial: it is easily removed after processing. Moreover, epitaxied domains of P3HT can be obtained on various substrates, e.g., silicon wafers, ITO, and glass. The main difference lies in the ionic nature of the substrate used to grow epitaxially the P3HT film. The K−BrBz substrate is particularly interesting because (i) it is insoluble in organic solvents such as chloroform and chlorobenzene and (ii) it is infusible at the melting temperature of P3HT (T_m = 240 °C). Therefore, it is possible to perform the isothermal crystallization of the P3HT films after a preliminar melting step that erases the initial structure of the solution cast films.

As seen in the Supporting Information (Figure S2), the specular scan of K−BrBz crystalline films formed by slow evaporation on a glass substrate shows the full sequence of (h 0 0) reflections with h = 4, 8, 12, and 14 suggesting a preferential $(1\,0\,0)_{K-BrBz}$ contact plane. The crystal structure of K−BrBz consists of a polar−apolar sandwich arrangement based on two layers of the 4-bromobenzoate molecules linked by one layer of potassium ions.[21,22] Cleavage occurs mainly between the successive planes of benzoate molecules separated by bromine atoms. Accordingly, the surface of K−BrBz crystals is a nearly rectangular array with parameters b_{K-BrBz} = 0.389 nm, c_{K-BrBz} = 1.12 nm, and β = 89.9°.

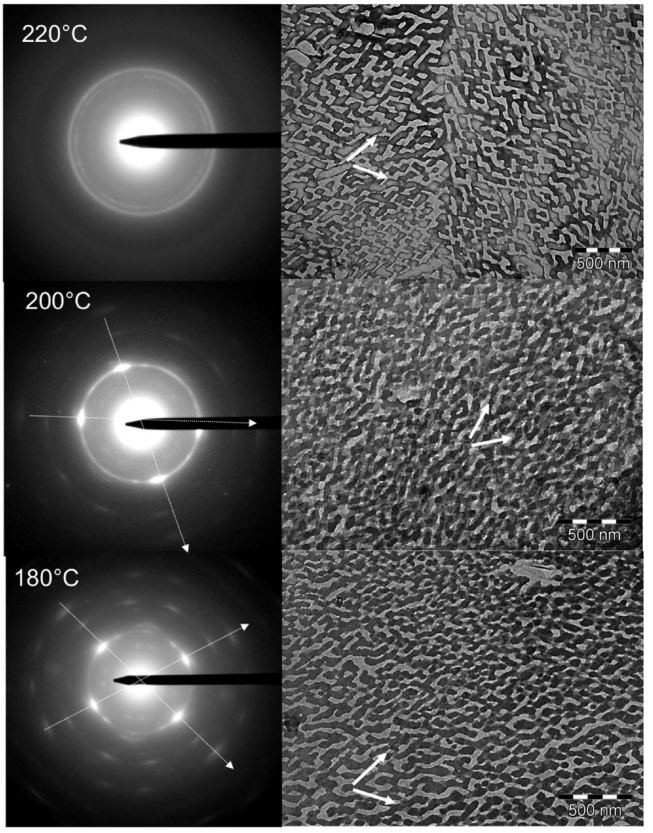

Figure 2. Evolution of the thin film structure and morphology in isothermally crystallized P3HT thin films grown on K−BrBz substrates for various crystallization temperatures in the range 180 °C-220 °C. The two arrows in the ED pattern highlight the two preferential in-plane orientations of the b_{P3HT} axis.

A remarkable feature of this substrate is the existence of rows of bromine atoms separated by 0.56 nm running parallel to b_{K-BrBz}. The large $(1\,0\,0)_{K-BrBz}$ surfaces can accordingly be used as substrates for the epitaxial crystallization of P3HT.

As illustrated in Figure 1, parts b and c, the epitaxied P3HT areas on single-crystalline surfaces of K−BrBz show some anisotropy of the optical absorbance which is indicative of in-plane orientation of the P3HT film. Nevertheless, the dichroism in optical absorbance is much lower than for the P3HT films oriented by directional epitaxial crystallization on TCB. This observation is consistent with the existence of two in-plane orientations of the P3HT chain axis (vide infra) rather than a single in-plane orientation as observed for the P3HT films oriented on TCB. As a matter of fact, when K−BrBz crystallizes in the form of lozenge-shaped crystals, the contours of the epitaxied P3HT areas correspond to those of the initial K−BrBz crystals. This is clearly observed in the bright field TEM image of Figure 1d showing the lozenge-shaped area of an epitaxied P3HT film. P3HT areas not covered by the K−BrBz crystals do not show any nanotexturing (see Figure 1d).

b. Effect of Isothermal Crystallization Temperature. In a first set of experiments, the impact of isothermal crystallization temperature T_{iso} and duration on the morphology and structure of the epitaxied P3HT films was analyzed. Figure 2 depicts the evolution of the P3HT film morphology (TEM bright field) and of the corresponding electron diffraction (ED) pattern as a function of T_{iso}. The impact of T_{iso} on the crystallinity and film morphology is crucial. For P3HT films annealed at 220 °C, the ED pattern shows two Scherrer rings corresponding to reticular distances of 0.39 nm

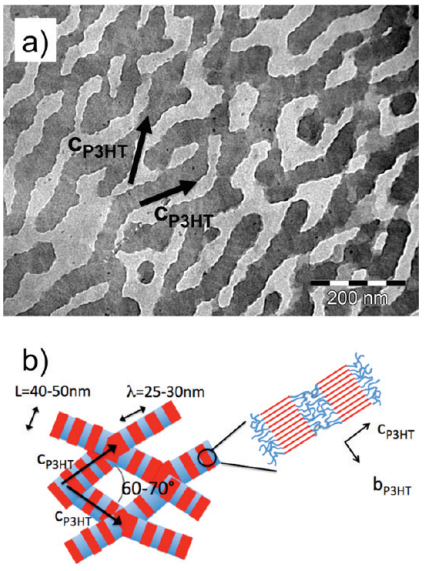

Figure 3. (a) Bright field TEM image of an oriented P3HT film grown on the 1 0 0 crystal surface of K−BrBz at 180 °C. Note the alternation of dark and brighter stripes in the oriented domains. The two preferential in-plane orientations of the P3HT chains (c_{P3HT}) are depicted by two arrows. (b) Scheme showing the organization of the nanostructured P3HT films grown on K−BrBz substrate. Crystalline zones are shown in red while amorphous interlamellar zones are colored in blue.

(indexed as 0 2 0) and 0.43 nm. The morphology is nanostructured with lozenge-shaped domains running along two preferential orientations of the substrate plane. The edges of the lozenge-shaped domains make an acute angle of approximately 55 deg. The typical size of the nanostructured domains is in the range 50−100 nm. The overall film texture suggests that the P3HT film has decorated and templates a nanostructured and textured K−BrBz surface.

For T_{iso} = 200 °C, both the morphology and the structure of the films change substantially. The uniform Scherrer ring corresponding to the 0 2 0 reflection decreases in intensity and overlaps with four very intense reflections along two in-plane directions making a relative angle of 70 ± 1 deg. Additional reflections of weaker intensity are also observed, suggesting that the overall crystallinity of the samples annealed at 200 °C is substantially higher than for 220 °C. Consistently with the ED pattern, the film morphology is now a highly interconnected network of domains with two major in-plane orientations. However, the P3HT films cover only about 50% of the K−BrBz surface.

When annealing of the P3HT films is performed at T_{iso} = 180 °C, the Scherrer ring of the 0 2 0 reflection is replaced by a pattern of extremely sharp reflections indicating a very high level of crystallinity and two well-defined in-plane orientations of the P3HT domains. Again, the 2-fold in-plane orientation of the P3HT domains on the K−BrBz substrate is apparent in the nanotextured morphology of the films (see Figure 2). Careful inspection of the TEM bright field shown in Figure 3a reveals interesting aspects of the morphology of the P3HT films grown at T_{iso} = 180 °C. The P3HT nanodomains show a remarkable internal nanostructuring which is manifested by the periodic alternation of dark and bright stripes with a periodicity of 25−30 nm. The darker stripes correspond to the diffracting, i.e., crystalline lamellae of the polymer. These stripes are oriented perpendicular to the long axis of the P3HT domains (see scheme in Figure 3). A similar organization was observed in the epitaxied P3HT films grown by directional epitaxial crystallization on TCB.[11,12] In the semicrystalline structure of P3HT, crystalline lamellae

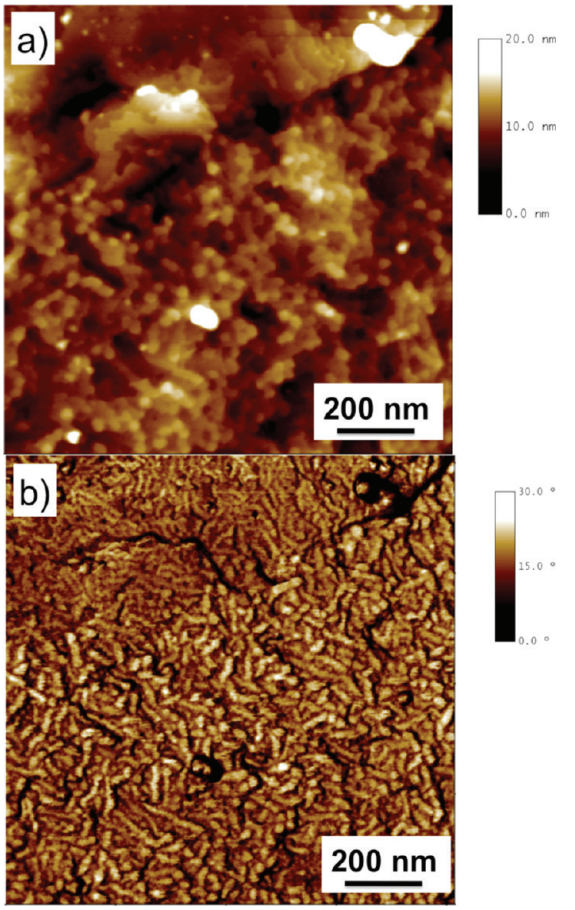

Figure 4. Surface structure of oriented and nanotextured P3HT films crystallized on top of a K−BrBz substrate at T_{iso} = 180 °C, observed by ATM in (a) topography mode and (b) phase mode.

alternate with amorphous interlamellar zones and the chain direction is on average perpendicular to the lamellar surface. Further evidence for the semicrystalline structure of the P3HT domains is obtained by TEM dark field imaging. In Figure S3 (Supporting Information), we show the ED pattern and the corresponding DF and BF images of a P3HT film grown on K−BrBz at T_{iso} = 180 °C. The DF image was obtained by selecting one of the 0 2 0 reflections corresponding to one preferred in-plane orientation of the P3HT crystals. The DF image shows bright and narrow stripes elongated in the direction of the selected 0 2 0 reflection i.e. the direction perpendicular to the P3HT chain direction. Accordingly, the isothermal crystallization of P3HT at 180 °C on K−BrBz leads to the organization illustrated schematically in part b of Figure 3. The films are made of highly interconnected and elongated semicrystalline stripes with an average width of 50−100 nm. Within the P3HT stripes, oriented crystalline domains alternate with amorphous interlamellar zones. The chain axis direction within the stripes is oriented in the direction perpendicular to the alternating dark and bright stripes, i.e., along the two in-plane growth directions of the P3HT domains identified in the corresponding ED pattern.

The AFM topographic image and the phase-mode image also show the existence of preferential in-plane growth directions as seen in Figure 4. The upper part of the topographic image in Figure 4a shows the terraces of the K−BrBz substrate on top of which the P3HT film was grown by epitaxy. The phase-mode image in Figure 4 indicates that a very thin layer of oriented P3HT covers the terraces of the K−BrBz substrate although no clear feature is apparent in the corresponding topographic image. In the lower part of both images, the P3HT film is thicker and it shows a regular nanotextured morphology but with a layered structure corresponding most presumably to successive $(1\,0\,0)_{P3HT}$ planes (vide infra). Consistently with the morphological observations, the electron diffraction pattern reflects the existence of two in-plane orientations.

c. Identification of the P3HT Contact Plane. The ED pattern for the sample annealed at 180 °C is analyzed in detail in Figure 5. The complex diffraction pattern indicates two in-plane orientations of the semicrystalline P3HT domains as illustrated in Figure 5b. The ED pattern corresponding to one of the two populations is shown in Figure 5c. The reflection with the strongest intensity is indexed as 0 2 0 (0.39 nm) and corresponds to the period of π-stacking along the $\mathbf{b}_{P3HT}$ axis. Using the crystal structure of P3HT determined by electron diffraction analysis in reference 14, all the reflections are indexed as (0 k l) i.e. they belong to the $[1\,0\,0]_{P3HT}$ zone. The calculated ED pattern for this zone is shown in Figure 5d.

Both patterns in parts c and d of Figure 5 agree very well which supports the structural model of P3HT proposed in our previous study.[14] In particular, Figure 5c shows the remarkable absence of the 0 0 4 reflection whereas the 0 0 6 reflection is present. This peculiar feature of the ED pattern with a $[1\ 0\ 0]_{P3HT}$ zone has been considered as a characteristic fingerprint of the structural model proposed in our previous study, especially regarding the orientation of the *n*-hexyl side chains with respect to the polythiophene backbone. To conclude, the analysis of the ED pattern demonstrates that the P3HT lamellae grow exclusively with a $(1\ 0\ 0)_{P3HT}$ contact plane on the K−BrBz substrate and two in-plane orientations making a relative angle of 70° as illutrated in Figure 5.

d. Origin of the Oriented and Nanotextured Structure of the P3HT Films. The K−BrBz substrate has been used previously to orient form I′ of poly(1-butene).[21] Similarly to the case of P3HT, two in-plane orientations of the polymer chains were observed. The two orientations were explained in terms of 1D epitaxy based on the match between the interturn period of the poly(1-butene) helices and the repeat period between successive rows of bromine atoms. A comparable analysis was performed in the case of P3HT. As a matter of facts, the unit cell parameter b_{K-BrBz} is actually very close to the interchain chain π-stacking distance $b_{P3HT}/2$. Nevertheless, our experiments show that neither b_{P3HT} nor $\mathbf{c}_{P3HT}$ are oriented parallel to $\mathbf{b}_{K-BrBz}$. A first clue to explain the two in-plane orientations of P3HT chains on the KBrBz substrate is provided by the analysis of the surface structure of the K−BrBz substrate depicted in Figure 6. The $(1\,0\,0)_{K-BrBz}$ cleavage surface shows rows of bromine atoms running along the $\mathbf{b}_{K-BrBz}$ direction with a period of 0.56 nm. Interestingly, rows of bromine atoms run also along the $[0\ 2\ 1]_{K-BrBz}$ and the $[0\ -2\ 1]_{K-BrBz}$ directions. The relative angle between these two directions is 70 deg., i.e., it matches perfectly the observed angle between the two in-plane directions of the $\mathbf{c}_{P3HT}$ axis. Accordingly, the orientation relation at the P3H*T*/K−BrBz interface can be rationalized as follows:

$$(100)_{P3HT}//(100)_{K-BrBz} \quad (1)$$

and

$$[001]_{P3HT}//[0\ \pm\ 2\ 1]_{K-BrBz} \quad (2)$$

Attempts to find 1D or 2D epitaxial relations to account for the observed orientations of the P3HT domains on the

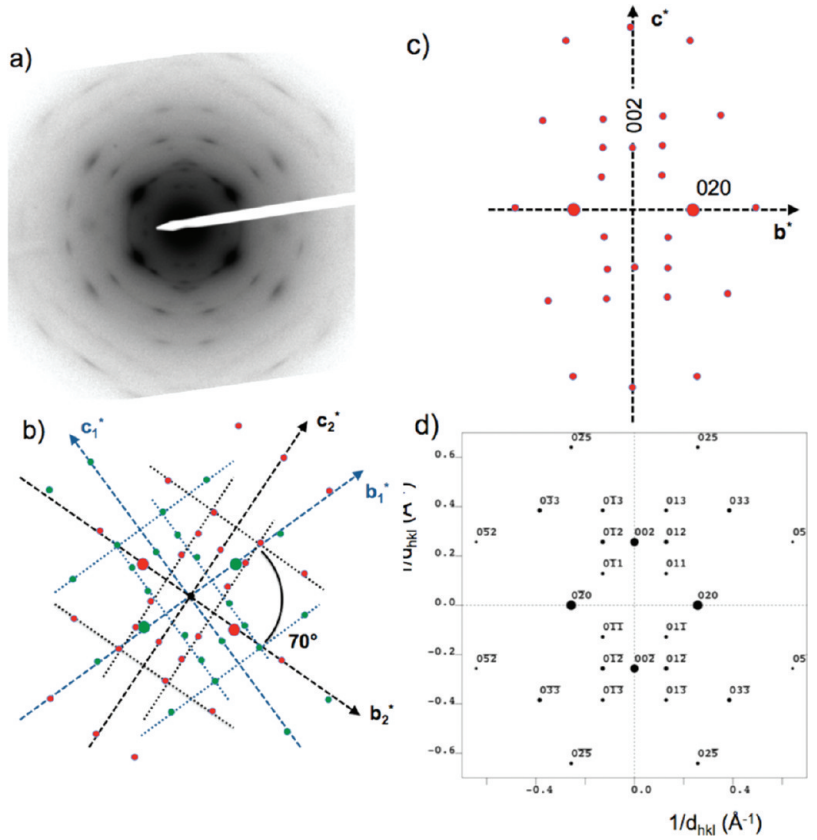

Figure 5. (a) ED pattern of an oriented P3HT thin films grown on KBrBz and annealed at 180 °C for 10 h. (b) Rationale of the experimental ED pattern showing the overlap of two ED patterns corresponding to crystalline P3HT domains with a (1 0 0) contact plane on the substrate and tilted at 70° one from another. (c) Single ED pattern and (d) calculated ED pattern using the crystal structure as determined in ref 14. Note the excellent agreement between both calculated and experimental ED patterns.

K−BrBz substrate by using the room temperature unit cell parameters of K−BrBz and P3HT failed. This is not surprising because the periodic order of P3HT is substantially altered at the isothermal crystallization temperatures used in our process (160−220 °C). Whereas the layered structure of π-stacked polythiophene backbones separated by layers of disordered *n*-hexyl side chains is maintained up to temperatures of 180−200 °C, the periodic order along the chain axis is lost because of conformational disorder of the conjugated polythiophene backbone.[23,24]

One key to the understanding of the orientation and nanotexturing mechanisms is given by the film morphology observed for T_{iso} = 220 °C. The P3HT domains are observed to form rhombic-shaped structures with a typical acute angle of 55 ± 4 deg. This angle matches the value expected between the $[0\ 1\ 0]_{K-BrBz}$ and the $[0\ 2\ 1]_{K-BrBz}$ directions on the K−BrBz substrate. Accordingly, the edges of the P3HT domains obtained at T_{iso} = 220 °C run either along the $[0\ 1\ 0]_{K-BrBz}$ or the $[0\ \pm2\ 1]_{K-BrBz}$ directions. This observation suggests that the in-plane orientation of the P3HT chains on the $(b,c)_{K-BrBz}$ plane is influenced by the surface structure of the K−BrBz crystals i.e. the presence of terraces with steps running in certain directions.

To check this hypothesis, we observed both the structure of the K−BrBz crystals before and after thermal annealing using the same conditions used for the P3HT thin film crystallization (240 °C for 1 min and 10 h at 180 °C). The AFM images of the as-grown K−BrBz substrates show a terraced structure. The smallest terrace height is in the range 1.5−1.7 nm which corresponds to $a_{K-BrBz}/2$ and is compatible with the preferential $(1\ 0\ 0)_{K-BrBz}$ orientation observed by X-ray diffraction. For the as-cast K−BrBz films, the terrace edges are irregular and do not correspond to preferential crystallographic directions. The surface morphology of the annealed K−BrBz substrates is substantially modified as seen in Figure S4b of the Supporting Information. The K−BrBz crystals annealed for 10 h at 180 °C show a "hill-and-valley" surface with a typical depth of the "valleys" of approximately 50 nm and a width in the range 30−70 nm. Some of the surface features resemble the etch pits formed on the surface of organic crystals, e.g., the {0 1 0} surface of potassium acid phthalate.[25] As seen in Figure S4b, the rhombic shape of certain etch pits show identical characteristics with those observed in Figure 2 for the rhombic-shaped P3HT domains. The edges of the valleys seem to run along two preferential in-plane directions making a relative angle of 70 ± 5 deg. This angle corresponds closely to the angle between the $[0\ 2\ 1]_{K-BrBz}$ and the $[0\ -2\ 1]_{K-BrBz}$ directions i.e the step edges of the K−BrBz substrate are oriented along these two preferential directions. A closer look at the "reconstructed" surface (see Figure S4c) indicates that the step edges are not irregular but seem to follow certain crystallographic directions of the K−BrBz crystal similarly to the deeper valleys. In addition, the typical size of the K−BrBz valleys is in accordance with that of the oriented P3HT domains seen in Figures 2 and 3. All together, these observations indicate that the P3HT nanotexturing is the result of the surface reconstruction of the K−BrBz crystals and that the in-plane orientation of the P3HT chains is given by the orientation of the step edges, i.e., the $[0\ 2\ 1]_{K-BrBz}$ and the $[0\ -2\ 1]_{K-BrBz}$ directions.

The buildup of ordered nanotextured morphologies has been observed in a number of cases, e.g., for gold thin films on a reconstructed alumina surface.[26,27] For instance, the

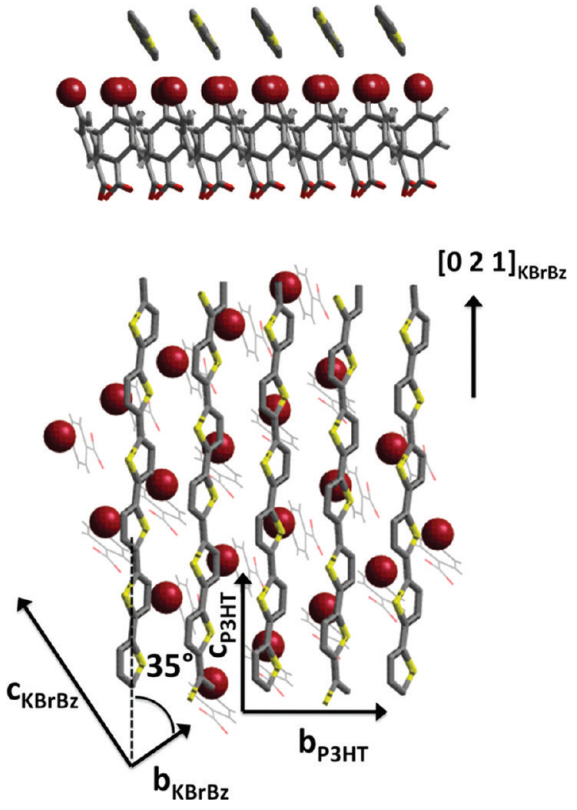

Figure 6. Molecular model of the interface between the K−BrBz substrate and the crystalline P3HT. For the sake of clarity, only the conjugated backbone of the P3HT has been shown. The Bromine atoms of the 4-bromobenzoate are shown as magenta balls. The top image corresponds to a projection perpendicular to the rows of bromine atoms running along the $[0\ 2\ 1]_{K-BrBz}$ direction whereas the lower one shows the projection of the interface along the normal to the substrate plane. Note the orientation of the P3HT chains parallel to the rows of bromine atoms along the $[0\ 2\ 1]_{K-BrBz}$ direction.

"hill-and-valley" or "factory-roof" structure of a (1 0 −1 0) alumina surface can generate regular arrays of Au nanowires upon thermal annealing at 800 °C. The gold nanowires are preferentially located in the valleys of the reconstructed alumina substrates. A similar situation is very likely to occur in the present case; the growth of P3HT crystalline domains is confined to the valleys of the reconstructured K−BrBz surface.

A further argument explaining the efficient nucleation and orientation of P3HT crystals by the "reconstructed" K−BrBz surface lies in the fact that the average terrace height of the K−BrBz substrate matches closely the periodicity of the layered structure of P3HT. Indeed, as demonstrated by Tashiro et al. on oriented P3HT films, the lamelar period a_{P3HT} tends to increase substantially up to a value of 1.75 nm at 180°C. This value matches almost perfectly the observed terrace height of the K−BrBz substrate, i.e., $a_{K-BrBz}/2 = 1.745$ nm. This correspondance suggests that the preferential orientation of the P3HT chains occurs at the step edges of the K−BrBz crystals which help to align the P3HT chains and nucleate successive layers of P3HT chains as illustrated in Figure 7. The selection of the in-plane orientation of P3HT chains follows the two preferential directions $[0\ \pm2\ 1]$ of the step edges. The progressive loss of the preferred in-plane orientation of the P3HT domains observed for $T_{iso} \geq 200$°C can also be explained on the basis of the results of Tashiro et al.[23] Indeed, as seen in Figures 9 and 10 of ref 23, the intensity of the (h 0 0) reflections is decreasing drastically for T ≥ 200°C. This

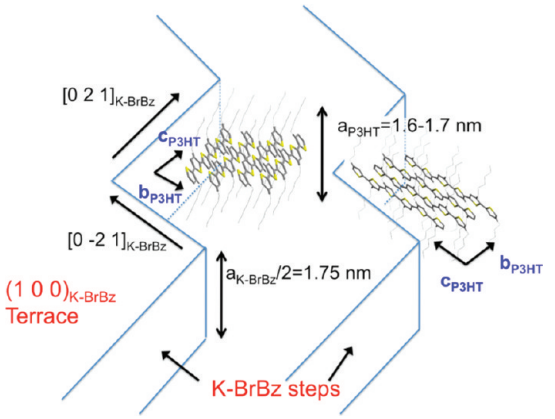

Figure 7. Schematic representation of the preferential nucleation and orientation of P3HT crystalline domains at the steps of a reconstructed K−BrBz substrate. The P3HT chains are running parallel to the $[0\ 2\ 1]_{K-BrBz}$ or the $[0\ -2\ 1]_{K-BrBz}$ directions. The height of the π-stacked P3HT chains matches closely the observed step height of the K−BrBz substrate.

indicates that for T ≥ 200°C, the "smectic"-like structure of P3HT implying layers of π-stacked polythiophene backbones separated by layers of disordered *n*-hexyl side-chains is lost. Accordingly, it is the absence of a well-defined layered structure of P3HT for $T \geq 200$°C that prevents achieving a high in-plane orientation of the P3HT domains. However at these high temperatures, the "hill and valley" surface of the K−BrBz substrate still acts as a nanostructured template for the growth of the rhombic-shaped P3HT domains but without inducing a preferential in-plane orientation of the polymer chains.

To a certain extent, the present orientation mechanism for $T_{iso} \leq 200$ °C bears some smilarity with so-called grapho-epitaxial orientation[28] but the main difference is that the molecular structure of the K−BrBz substrate is essential for the efficient nucleation of P3HT crystalline domains at temperatures below 180 °C. As a matter of fact, attempts to orient other poly(3-alkylthiophenes), e.g., poly(3-butylthiophene) and poly(3-decylthiophene), at different isothermal crystallization temperatures on the K−BrBz substrate were not successful. This is consistent with the fact that the layer period of these P3ATs does not match the step height of the K−BrBz substrate (at room temperature, P3DT is characterized by a layer period of 2.0 nm vs 1.3 nm for P3BT). The orienting and nucleating role of substrate ledges on the surface of molecular crystals used as substrates for the growth of organic molecules has been previously pointed out by Ward and co-workers.[29] It was proposed that the match between the substrate ledge and the overlayer aggregate geometries can explain the preferential nucleation of the deposited molecules at ledge sites. Moreover, the free energy for nucleation at ledge sites is substantially lowered as compared to the nucleation on a flat featureless surface. Ledge-directed nucelation and growth was observed in the case of benzoic acid growing on L-valine substrates.[30] Brinkmann and co-workers suggested that a similar mechanism could explain the orientation of certain conjugated molecular materials e.g. pentacene, titanyl phthalocyanine and conjugated polymers like poly(9,9-bis(2-ethylhexyl)fluorene-2,7-diyl) on substrates of poly(tetrafluoroethylene).[16,31,32] The present results provide strong evidence that such a mechanism is also at play in the case of P3HT on a K−BrBz substrate. However, in the present case, the original aspect of the growth mechanism is that the nanotexturing of the oriented polymer layer is the consequence of a topographic "reconstruction" of the substrate surface. Reconstruction of

a metallic gold substrate upon deposition of conjugated molecules has been reported,[33] but to the best of our knowledge, no such effect has been evidenced in the case of a polymer deposited on an aromatic substrate. One may wonder if the regular nanotexturing of the P3HT film could not be the result of a synergetic mechanism that associates the surface "reconstruction" of K−BrBz and the isothermal crystallization of the polymer. The P3HT film may enhance the efficency of the topographic reconstruction of the K−BrBz crystal surface by imparting a higher mobility to the benzoate molecules and potassium ions at step edges during the isothermal crystallization of the polymer. On the one hand, the layer of P3HT would help nanostructuring the K−BrBz substrate surface. On the other hand, the reconstructed K−BrBz surface would act as a nanostructured template for the oriented growth of crystalline P3HT domains. The synergy between P3HT crystallization and surface reconstruction of K−BrBz is further supported by the regularity of the nanotextured P3HT films in terms of length scale.

Conclusion

Highly oriented and nanotextured P3HT thin films made of a network of interconnected semicrystalline domains oriented along two preferential in-plane directions have been obtained by an original growth mechanism involving the reconstructed surface of an aromatic substrate. Isothermal crystallization of regioregular poly(3-hexylthiophene) (P3HT) on potassium 4-bromobenzoate (K−BrBz) crystals can generate extended patterns of highly interconnected crystalline P3HT domains oriented along the $[0 \pm 2\ 1]_{K-BrBz}$ directions corresponding to rows of bromine atoms on the K−BrBz substrate and a unique $(1\,0\,0)_{P3HT}$ contact plane. The P3HT film morphology mimics the reconstructed K−BrBz surface showing a regularly nanostructured "hill-and-valley" topography at a 50−100 nm length scale. Nucleation of oriented P3HT domains occurs at the step edges of the K−BrBz substrate oriented along two preferential in-plane directions ($[0 \pm 2\ 1]_{K-BrBz}$). This nucleation is further favored by the fact that the average height of the $(1\ 0\ 0)_{K-BrBz}$ substrate terraces matches the layer period of π-stacked P3HT chains. The regularity of the P3HT patterns in terms of length scale supports a growth mechanism that associates the substrate surface "reconstruction" and the epitaxial crystallization of the polymer. Such nanotextured and highly crystalline P3HT films could be of interest for the elaboration of active layers with a nanostructured bulk heterojunction morphology used in organic solar cells.

Acknowledgment. Enlightening discussions with Dr. Bernard Lotz are gratefully acknowledged. Financial support was provided by the Agence Nationale de la Recherche under Contract ANR-08-NANO-012-01.

Supporting Information Available: Figures showing powder diffraction spectra, electron diffractions patters, and the effect of anneling on the surface morphology. This material is available free of charge via the Internet at http://pubs.acs.org.

References and Notes

(1) Sirringhaus, H.; Brown, P. J.; Friend, R. H.; Nielsen, M. M.; Bechgaard, K.; Langeveld-Voss, B. M. W.; Spiering, A. J. H.; Janssen, R. A. J.; Meijer, E. W.; Herwig, P.; de Leeuw, D. M. *Nature* **1999**, *401*, 685–688.
(2) Salleo, A. *Mater. Today* **2007**, *10*, 38.
(3) Peet, J.; Heeger, A. J.; Bazan, G. C. *Acc. Chem. Res.* **2009**, *42*, 1700.
(4) Lindner, S. M.; Huettner, S.; Chiche, A.; Thelakkat, M.; Krausch, G. *Angew. Chem., Int. Ed.* **2006**, *45*, 3364.
(5) Scherf, U.; Gutacker, A.; Koenen, N. *Acc. Chem. Res.* **2008**, *41*, 1086.
(6) Castro, F. A.; Benmansour, H.; Graeff, C. F. O.; Nüesch, F.; Tutis, E.; Hany, R. *Chem. Mater.* **2006**, *18*, 5504.
(7) Zhang, F.; Nyberg, T.; Inganäs, O. *Nano Lett.* **2002**, *2*, 1373.
(8) Cavallini, M.; Albonetti, C.; Biscarini, F. *Adv. Mater.* **2009**, *21*, 1043.
(9) Hu, Z.; Muls, B.; Gence, L.; Serban, D. A.; Hofkens, J.; Melinte, S.; Nysten, B.; Demoustier-Champagne, S.; Jonas, A. M. *Nano Lett.* **2007**, *7*, 3639.
(10) Jimison, L. H.; Toney, M. F.; McCulloch, I.; Heeney, M.; Salleo, A. *Adv. Mater.* **2009**, *21*, 1568.
(11) Brinkmann, M.; Wittmann, J.-C. *Adv. Mater.* **2006**, *18*, 860.
(12) Brinkmann, M.; Rannou, P. *Adv. Funct. Mat.* **2007**, *17*, 101.
(13) Brinkmann, M.; Rannou, P. *Macromolecules* **2009**, *42*, 1125.
(14) Kayunkid, N.; Uttiya, S.; Brinkmann, M. *Macromolecules* **2010**, *43*, 4961.
(15) Brinkmann, M. *Macromolecules* **2007**, *40*, 7532.
(16) M. Brinkmann, M.; Charoenthai, N.; Traiphol, R.; Piyakulawat, P.; Wlosnewski, J.; Asawapirom, U. *Macromolecules* **2009**, *42*, 8298.
(17) Wittmann, J. C.; Lotz, B. *J. Polym. Sci., Polym. Phys.* **1981**, *19*, 1837–1851.
(18) Wittmann, J. C.; Lotz, B. *J. Polym. Sci., Polym. Phys.* **1981**, *19*, 1853–1864.
(19) Wittmann, J. C.; Hodge, A. M.; Lotz, B. *J. Polym. Sci., Polym. Phys.* **1983**, *21*, 2495–2509.
(20) Wittmann, J. C.; Lotz, B. *Prog. Polym. Sci.* **1990**, *15*, 909–948.
(21) Kopp, S.; Wittmann, J. C.; Lotz, B. *Polymer* **1994**, *35*, 916.
(22) Mills, H. H.; Speakman, J. C. J. *J. Chem. Soc.* **1963**, 4355.
(23) Tashiro, K.; Ono, K.; Minagawa, Y.; Kobayashi, M.; Kawai, T.; Yoshino, K. *J. Polym. Sci., B: Polym. Phys.* **1991**, *29*, 1223.
(24) Causin, V.; Marega, C.; Margio, A.; Valentini, L.; Kenny, J. M. *Macromolecules* **2005**, *38*, 409.
(25) (a) Woensdregt, C. F.; Glikin, A. E. *J. Cryst. Growth* **2005**, *283*, 523. (b) Uthayarani, K.; Sankar, R.; Shashidharan Nair, C. K. *Cryst. Res. Technol.* **2008**, *43*, 733.
(26) Basu, J.; Carter, B.; Divakar, R.; Mukherjee, B.; Ravishankar, N. *Appl. Phys. Lett.* **2009**, *94*, 171114.
(27) Saxena, R.; Frederick, M. J.; Ramanath, G.; Gill, W. N.; Plawsky, J. L. *Phys. Rev. B* **2005**, *72*, 115425.
(28) Givargizov, E. I. In *Artificial Epitaxy* (*Graphoepitaxy); Hand-book of Crystal Growth*; Hurle, D. T. J., Ed.; Elsevier Science: New York, 1994; Vol. *3*.
(29) Ward, M. D. *Chem. Rev.* **2001**, *101*, 1697.
(30) Carter, P. W.; Ward, M. D. *J. Am. Chem. Soc.* **1993**, *115*, 11521.
(31) Brinkmann, M.; Graff, S.; Wittmann, J.-C.; Chaumont, C.; Nuesch, F.; Anver, A.; Schaer, M.; Zuppiroli, L. *J. Phys. Chem. B* **2003**, *107*, 10531.
(32) Brinkmann, M.; Wittmann, J.-C.; Barthel, M.; Hanack, M.; Chaumont, C. *Chem. Mater.* **2002**, *14*, 936.
(33) Evangelista, F.; Ruocco, A.; Pasca, D.; Baldacchini, C.; Betti, M. G.; Corradini, V.; Mariani, C. *Surf. Sci.* **2004**, *566*, 79.